Published in IET Computer Vision
Received on 29th October 2010
Revised on 31st August 2011
doi: 10.1049/iet-cvi.2010.0191

Special Issue: Future Trends in Biometric Processing

ISSN 1751-9632

Towards contactless palmprint authentication

A. Morales[1,2] *M.A. Ferrer*[1] *A. Kumar*[2]

[1]*Instituto Universitario Para el Desarrollo Tecnológico y la Innovación en Comunicaciones (IDeTIC), Universidad de Las Palmas de Gran Canaria, Campus de Tafira, E35017 Las Palmas de Gran Canaria, Spain*
[2]*Department of Computing, The Hong Kong Polytechnic University, Hung Hom, Hong Kong, Kowloon, People's Republic of China*
E-mail: amorales@gi.ulpgc.es

Abstract: This study examines the issues related to two of the most palmprint promising approaches applied to the contactless biometric authentication and presents a performance evaluation on three different scenarios. The presence of significant scale, rotation, occlusion and translation variations in the contactless palmprint images requires the feature extraction approaches that can accommodate such within class image variations. Therefore the usage and performance of traditional palmprint feature extraction methods on contactless imaging schemes remain questionable and hence all/popular palmprint feature extraction methods may not be effective in contactless frameworks. The experimental results on more than 6000 images from three contactless databases acquired in different environments suggest that the scale invariant feature transform (SIFT) features perform significantly better for the contactless palmprint images than the promising orthogonal line ordinal features (OLOF) approach employed earlier on the more conventional touch-based palmprint imaging. The experimental results further suggest that the combination of robust SIFT matching scores along with those from OLOF can be employed to achieve more reliable performance improvement. The use of publicly available databases ensures repeatability in the experiments. Therefore this study provides a new/challenging contactless hand database acquired in uncontrolled environments for further research efforts.

1 Introduction

The hand-based biometric identification systems have traditionally been based on peg guide [1] or the recently explored more convenient peg-free hand imaging systems [2]. Therefore the contact between user and device is inevitable. The deployment of such devices with large number of users, for example, airport access as during the earlier USVISIT program, raises hygienic concerns. The usage of contactless acquisition devices emerges as the obvious solution to alleviate such hygienic concerns. The absence of contact improves the user convenience but results in large image variations which require robust algorithms to accommodate such variations.

The main difference between contact-based and contactless systems lies in the significant intra-class variations resulting from the absence of any contact or guiding surface to restrict such variations. Such variations can result from the rotational and translation variations, projective distortion, scale variations and blurring due to the hand movement during the image acquisition. The first challenge is therefore to employ better image normalisation while the key research challenge is to develop robust feature extraction and matching approaches which are invariant to such image variations from contactless imaging.

In recent years, there have been several efforts to develop robust approaches for contactless hand-based biometrics. Promising results were obtained using palm texture [3], palmvein [4] or hand geometry [5] on controlled environments. The simultaneous use of 3D and 2D hand information has been investigated in [6] to alleviate the projective distortion problems associates to the absence of a contact surface. The images were acquired in contactless condition in a controlled scenario. The elevated cost of the 3D scanners is prohibitive for its possible current deployment but it can be a possible solution in the near future. Traditionally, the control of illumination and background is achieved by black box schemes. The acquisition inside a black box to control the environmental conditions can raise concerns or unwillingly scare the users and reduce the user acceptance. The absence of public databases of contactless hand images acquired in uncontrolled environments is an important lack of the state-of-the-art.

This paper systematically investigates the application of the two most promising feature extraction approaches for the contactless palmprint identification [7]. The first approach using scale invariant feature transform (SIFT) is proposed to address the large intra-class variations from contactless imaging. SIFT was originally proposed for object recognition applications. Therefore we have developed modification to this approach using images preprocessing techniques and matches score generation to accommodate inherent image distortions from the contactless imaging. We also examine the performance from possibly the best approach (as shown in [8]) in the palmprint literature using orthogonal line ordinal feature (OLOF)-based feature extraction. The comparison between two such feature extraction methods adds to the existing knowledge for the performance from the contactless

palmprint identification. This paper provides new/challenging contactless hand database acquired in uncontrolled environments for further research efforts. Our experiments employ more than 6000 different images from three contactless databases acquired in controlled and uncontrolled environments conditions. These experimental results are significant and suggest that the modified SIFT approach performs significantly better than OLOF approach that performed best among the several competitive approaches in [8]. The experimentation in this paper provides more detailed explanation on scale, occlusion, rotation and translational tolerance capabilities and experimental illustrations from real contactless images to ascertain such promises. However, the features extracted from SIFT and OLOF are expected to be complimentary and therefore it is judicious to combine these two observations and ascertain the further improvement in the performance.

2 Databases

In this work, we used three contactless databases acquired in controlled and uncontrolled environmental conditions. The uncontrolled conditions refer to the acquisition of images in open conditions with background and surrounding illumination uncontrolled in the office environment. The use of publicly available databases in the performance evaluation ensures repeatability in the experiments and it is important for comparison with other approaches. In this paper we employed three databases; two of them are publically available for further research efforts.

The IITD touchless palmprint database is a publicly available database [9] and it consists of hand images with high projective, scale, rotational and translational variations. The database is composed of images from the left and right hands of 235 subjects. Considering each of the two hand images (left and right) as belonging to two independent users, we have 470 different hands images with a minimum number of 6 images per user. The database was acquired in single imaging sessions. As shown in Fig. 1, during the acquisition illumination and background conditions were quite controlled.

The GPDS-CL1 is a new publicly available database [10] acquired in the University of Las Palma de Gran Canaria which is composed by 10 images of the right hand of 100 subjects. The database was acquired in single session with uncontrolled background and illumination. Despite the single session image acquisitions, as can be seen in Fig. 1, the surrounding illumination conditions were varying even for the same user.

The GPDS-CL2 database, also from the University of Las Palmas de Gran Canaria, is a real application contactless database consisting of 110 subjects imaging with average number of images per subject as 14. This database is divided into two categories of users: habitual users and sporadic users; 70 habitual people used the system once per week during a 4-month period; this generated 10 sessions per user. The 40 sporadic people (those users who are not familiar to interact with the imaging device) were acquired in 2 or 3 sessions. The training phase was supervised and the test phase was unsupervised. We have not rejected any of the images from the 4-month experiments. Some examples of acquired images can be seen in Fig. 1. This database images show several pose, illumination and background variations.

The main objective in building this database is to have large number of sessions and the unsupervised conditions for the imaging. This attempts to represent more realistic application environment. However, the 110 subjects employed to build this database may not be enough to represent large population. In order to comparatively analyse the three databases, the differences and similarities between them are summarised in Table 1.

In terms of projective, scale and blurred variation, the GPDS-CL2 database shows a greater variations and distortions in the acquired images. The three databases are examples of two different imaging environments: laboratory environment and real/outdoor application environment.

3 Feature extraction

The images acquired in contactless schemes are often characterised with the presence of severe rotational scale

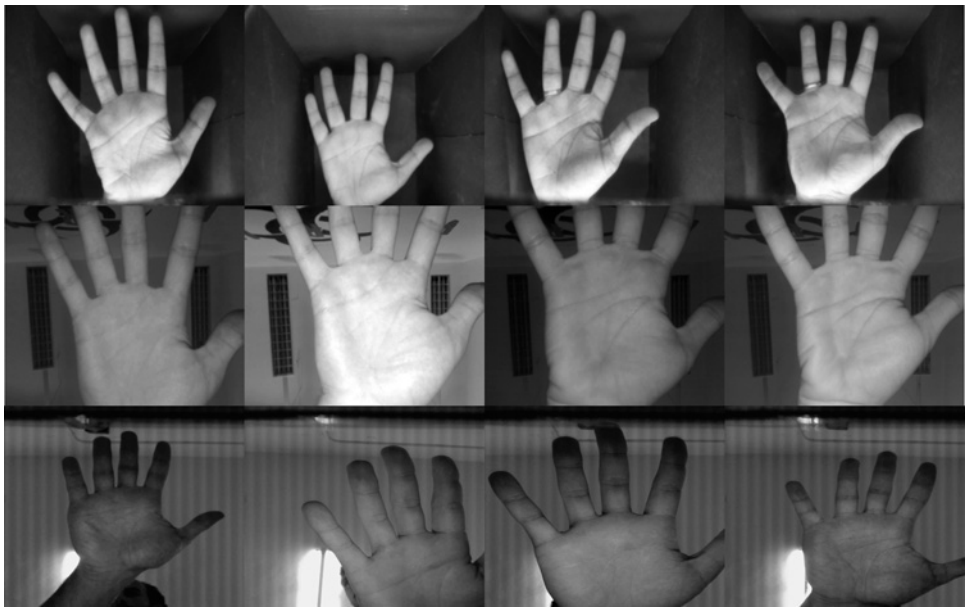

Fig. 1 *Images in first row are from two subjects in IITD touchless database while second and third row images are from two subjects in GPDS-CL1 and GPDS-CL2 database*

doi: 10.1049/iet-cvi.2010.0191

Table 1 Main characteristics of IITD and GPDS-CL1 and 2 databases

Characteristics	IITD	GPDS-CL1	GPDS-CL2
users	234	100	110
hand acquired	both	right	right
acquisitions per user	greater than 6	10	14
sessions	1	1	3–10
acquisition method	contactless supervised	contactless supervised	contactless unsupervised
background	controlled	uncontrolled	uncontrolled
illumination	controlled	uncontrolled	uncontrolled
image resolution	800 × 600	800 × 600	800 × 600

and translation changes, unlike those acquired from conventional systems based on the use of pegs or hand docking frame. Therefore the usage of traditional palmprint feature extraction methods remains questionable and hence all/popular palmprint feature extraction methods may not be effective in contactless frameworks. This section details the adaptation of classical OLOF and SIFT-based feature extractors to the contactless palmprint imaging problem.

The segmentation of region of interest, that is, palmprint, has been performed in different ways for each database. For IITD database the palmprint segmented images is provided along with the database. For GPDS-CL1 and CL2 databases the procedure is similar. The device acquires hand images in infrared and visible band illumination. The hand is easily segmented from the infrared images and the coordinates of the valleys between fingers are automatically located. Those coordinates are then mapped to the corresponding visible image and a translation and rotation invariant palmprint area is obtained following the procedure similar as described in [11]. In our work, we employ the contactless palmprint images of size 150 × 150 pixels for the feature extraction stage as described in next section.

3.1 Modified SIFT (MSIFT)

The SIFT was originally proposed in [12]. In [13] the utility of SIFT features for palmprint identification was examined with relatively poor results using images acquired from flat-bed scanner, which uses constrained imaging with user-pegs. The features extracted are invariant to image scaling, rotation and partially invariant to change in illumination and projective distortion. The SIFT is a feature extraction method based on the extraction of local information. Fig. 2 resumes the major stages to generate the set of features proposed by Lowe [12] and our proposal to adapt it to palmprint contactless biometric systems called MSIFT.

The SIFT algorithm is based on detecting keypoints with similar properties that are present in the reference and questioned image. In palmprint images are acquired contactless from hand on movement using complementary metal-oxide semiconductor (CMOS) sensors of low resolution (800 × 600), and the images include blurring and several above-mentioned distortions that reduce the ability of the SIFT algorithm to detect common keypoints. To alleviate such a problem, we propose a preprocessing that highlights the interesting keypoints. The algorithm that preprocesses the image obtained by previous application of the SIFT algorithm is called by us modified SIFT (MSIFT) and consists of six steps.

3.1.1 Preprocessing: In this paper we comparatively evaluate several preprocessing alternatives to add robustness

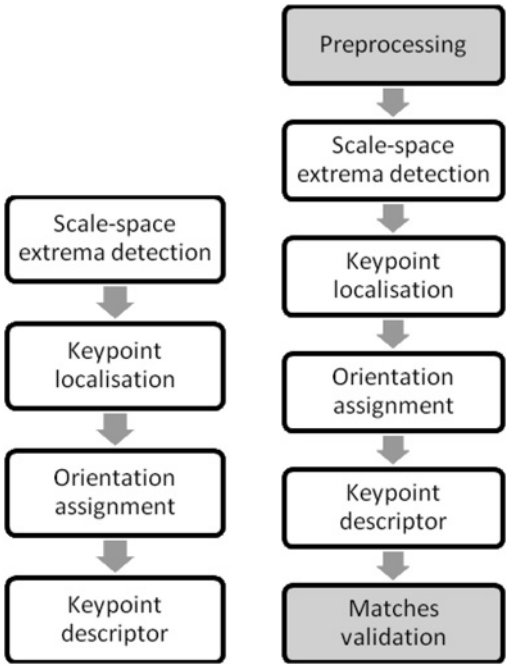

Fig. 2 *On the left the Lowe [12] SIFT approach; on the right the contactless palmprint MSIFT approach proposed on this paper*

to SIFT-based feature extraction approach: contrast limited adaptive histogram equalisation, Gaussian filtering and Gabor filtering. All of them assume that the reference and questioned hand have similar alignment inside the image which is true in our databases and is ensured during the segmentation stage.

The contrast limited adaptive histogram equalisation [14] is a preprocessing approach used to improve contrast in the images. For an input image $I(x, y)$, the cumulative distribution function is used to estimate the image histogram and a maximum desired slope to limit the contrast. The function is used to convert the greyscale density function into an approximately uniform density function.

The Gaussian filtering is based on 2D Gaussian filter to obtain the weighted average intensity of a line-like region. Its expression is as follows

$$f(x, y, \theta) = \exp\left[-\left(\frac{x\cos\theta + y\sin\theta}{\delta_x}\right)^2 - \left(\frac{x\sin\theta + y\cos\theta}{\delta_y}\right)^2\right] \quad (1)$$

where θ denotes the orientation of 2D Gaussian filter, δx denotes the filter's horizontal scale and δy denotes the filter's vertical scale parameter. We empirically selected the parameters as $\theta = 0$, $\delta_x = 5$ and $\delta_x = 1$.

The real 2D Gabor filter used to preprocess the palmprint image can be defined as follows

$$G(x, y, \theta, u, \varphi) = \frac{1}{2\pi\varphi^2}\exp\left\{-\frac{x^2 + y^2}{2\varphi^2}\right\} \times \cos\{2\pi(ux\cos\theta + uy\sin\theta)\} \quad (2)$$

where u is the frequency of the sinusoidal wave, θ defines the orientation selectivity of the function and φ is the standard deviation of the Gaussian envelope. In this paper we used a Gabor filter setting similar to the [14] proposal with $\varphi = 2$

and $u = 0.1$. Greater robustness against brightness variation is ensured by removing the average Gabor filter values from the discrete Gabor filter.

$$G'(x,\ y,\ \theta,\ u,\ \varphi) = G(x,\ y,\ \theta,\ u,\ \varphi) - \frac{\sum_{i=1}^{2n+1}\sum_{j=1}^{2n+1} G(i,\ j,\ \theta,\ u,\ \varphi)}{(2n+1)^2} \quad (3)$$

3.1.2 Scale-space extrema detection: It is employed over all scales and image locations. It is based on the difference-of-Gaussian function to identify potential interest points that are invariant to scale and orientation. The input data is transformed to the space $L(x, y, \sigma)$ as follows

$$L(x,\ y,\ \sigma) = g(x,\ y,\ \sigma) * I'(x,\ y) \quad (4)$$

where $*$ corresponds to convolution operator, $I'(x, y)$ is the preprocessed input image and $g(x, y, \sigma)$ is a Gaussian function with bandwidth σ. The difference-of-Gaussian function is defined as

$$\begin{aligned} D(x,\ y,\ \sigma) &= (g(x,\ y,\ k\sigma) - g(x,\ y,\ \sigma)) * I'(x,\ y) \\ &= L(x,\ y,\ k\sigma) - L(x,\ y,\ \sigma) \end{aligned} \quad (5)$$

3.1.3 Keypoint localisation: A detailed model is fit to determine location and scale of each candidate location. The interpolation is done using the quadratic Taylor expansion of the difference-of-Gaussian scale-space function $D(x, y, \sigma)$ with the candidate keypoint as the origin. This Taylor expansion is given by

$$D(x) = D + \frac{\partial D^{\mathrm{T}}}{\partial x} + \frac{1}{2}x^{\mathrm{T}}\frac{\partial^2 D^{\mathrm{T}}}{\partial x^2}x \quad (6)$$

where the maxima and minima of D and its derivatives are evaluated at the candidate keypoint and $x = (x, y, \sigma)$ is the offset from this point.

3.1.4 Orientation assignment: In our experiments we had used 16 orientations for each keypoint location based on local image gradient directions. For an image sample $L(x, y)$ at scale σ, the gradient magnitude, $m(x, y)$ and orientation, $\theta(x, y)$, are processed using pixel differences (see (7))

$$\theta(x,\ y) = \tan^{-1}\left(\frac{L(x,\ y+1) - L(x,\ y-1)}{L(x+1,\ y) - L(x-1,\ y)}\right) \quad (8)$$

3.1.5 Keypoint descriptor: Around each keypoint, the local gradients are measured at the selected scale to obtain a descriptors vector $\{d_i\}_{i=1}^{M}$ with M keypoints. Once the keypoints are extracted, the query image is matched and compared with each of the features extracted with the corresponding images in the registration database (from the training feature sets). The verifier evaluates the number of matches between a questioned and the training images. Let $\{d_i^{\mathrm{t}}\}_{i=1}^{M}$ and $\{d_i^{\mathrm{q}}\}_{j=1}^{L}$ be the set of training and questioned keypoint descriptors, respectively. The distance between keypoint descriptors is computed from the following

$$D_d(i,\ j) = \|d_i^{\mathrm{t}} - d_i^{\mathrm{q}}\|^2 \quad (9)$$

where $\|\cdot\|$ is the Euclidean norm. We define a match between a training d_i^{t} and a questioned d_i^{q} keypoint when

$$1.5D_d(i,\ j) < \min = \{D_d(i,\ j)\}_{n=1}^{L} \quad (10)$$

with $n \neq j$. The threshold is estimated heuristically during the training stage and it is not particularly sensitive to values in the range of 1.2–1.7.

3.1.6 Matches validation: The validation of matching scores for the authentication decisions is common in several other biometric feature extraction approaches. In this paper we propose a validation based on coordinates distance between keypoints to improve the SIFT performance on the contactless palmprint biometrics. The hypothesis is that the coordinates from two keypoints matched must be similar if we correct the average displacement from all the matches. Let $c_i^{\mathrm{t}} = \{x_i^{\mathrm{t}},\ y_i^{\mathrm{t}}\}_{i=1}^{M}$ and $c_i^{\mathrm{q}} = \{x_i^{\mathrm{q}},\ y_i^{\mathrm{q}}\}_{i=1}^{L}$ be the set of training and questioned keypoint coordinates, respectively. The distance between coordinates is calculated from the following

$$D_c(i,\ j) = \|c_i^{\mathrm{t}} - c_i^{\mathrm{q}}\|^2 \quad (11)$$

where $\|\cdot\|$ is the Euclidean norm. We define a match between a training c_i^{t} and a questioned c_i^{q} keypoint when

$$D_c(i,\ j) = \frac{1.5}{M}\sum_{i=1}^{M}\|c_i^{\mathrm{t}} - c_j^{\mathrm{q}}\|^2 \quad (12)$$

Owing to high pose variance in contactless imaging, we used a 1.5 weighting factor to accommodate small alignment errors between palms. The maximum number of matches between the questioned and the training set is the similarity score. If the similarity score is greater than a threshold, the questioned image is positively authenticated.

3.2 Orthogonal line ordinal features

The OLOF method was originally introduced in [8] and was investigated for the palmprint feature extraction. The comparison of OLOF method with several other competing methods [15–17] in this reference suggests the superiority of OLOF with such competitive feature extraction methods. The OLOF presented significantly improved results but on conventional databases that are acquired from constrained imaging.

The orthogonal filters are obtained using two Gaussian filters as follows

$$\mathrm{OF}(\theta) = f(x,\ y,\ \theta) - f\left(x,\ y,\ \theta + \frac{\pi}{2}\right) \quad (13)$$

Each palm image is filtered using three ordinal filters, OF(0), OF(π/6) and OF(π/3). In order to ensure the robustness against brightness, the discrete filters OF(θ), are turned to have zero average. The palmprint features are obtained

$$m(x,\ y) = \sqrt{(L(x+1,\ y) - L(x-1,\ y))^2 + (L(x,\ y+1) - L(x,\ y-1))^2} \quad (7)$$

doi: 10.1049/iet-cvi.2010.0191

filtering the palm image by the three ordinal filters, binarising the results with a threshold equal to zero, and resizing the binary image $n \times n = 50 \times 50$ pixels. An example of the feature matrix obtained using the three ordinal matrixes can be seen in Fig. 3.

The matching distance between the palmprint image feature matrix $Q = \{Q^{\theta=0}, Q^{\theta=\pi/6}, Q^{\theta=\pi/3}\}$ and the palmprint image feature matrix $P = \{P^{\theta=0}, P^{\theta=\pi/6}, P^{\theta=\pi/3}\}$ (i.e. reference and questioned templates) is computed by the normalised Hamming distance, which can be described as follows

$$D = (D^{\theta=0} + D^{\theta=\pi/6} + D^{\theta=\pi/3})/3 \tag{14}$$

being

$$D^{\theta} = 1 - \frac{\Sigma_{i=1}^{n}\Sigma_{j=1}^{n} P^{\theta}(i,\ j) \otimes Q^{\theta}(i,\ j)}{n^2} \tag{15}$$

where the Boolean operator $\otimes$ is the conventional XOR operator. The numeric value of D ranges between 0 and 1 and the best matching is observed when the value of D is 1. Because of the inherent intra-class variations in the contactless imaging and imperfections in preprocessing, the vertical and the horizontally translation ordinal feature map is used to ascertain the best possible matching score. The ranges of the vertical, horizontal translations and rotations are empirically determined and were fixed as from -6 to 6 (in the steps of two degrees). The maximum D value obtained from such multiple translated matching is assigned as the final matching score. If the final matching score is greater than a threshold, the training templates and the questioned images are authenticated as belonging to the same person.

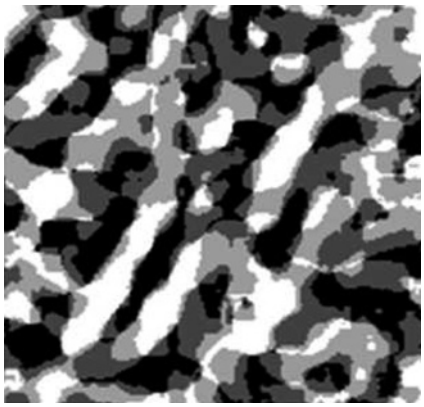

Fig. 3 *Ordinal feature image, OF(0) + OF(π/6) + OF(π/3), from a contactless palmprint image*

3.3 Matching score fusion

Combining scores obtained from different feature extraction approaches is a popular method of improving the performance for the multibiometrics identification. In this section we propose a method to determine the weights for the weighted combination of MSIFT and OLOF scores. Figs. 4 and 5 show the distribution of genuine and imposter matching scores from the two feature extraction approaches. We can ascertain that the matching scores from both the features are widely separated. The distribution of matching scores also suggests that the matching scores from the two matchers are likely to be uncorrelated and therefore more effectively employed for combination [18].

The OLOF and MSIFT scores were first normalised based on min–max approach [19]. The combined matching scores were generated using the weighted sum approach as follows

$$s_{\text{fusion}} = ws_{\text{MSIFT}} + (1 - w)s_{\text{OLOF}} \tag{16}$$

where s_{MSIFT} and s_{OLOF} are the scores obtained with MSIFT and OLOF features, w is the weighting factor and s_{fusion} is the combined score which will be used to verify the input identity.

The value of w is obtained as follows. Let $s^{\text{g}}_{\text{MSIFT}}(i)$ and $s^{\text{g}}_{\text{OLOF}}(i)$, $1 \le i \le N_g$ be the scores of the genuine training samples for MSIFT and OLOF approach, respectively. Let $s^{\text{f}}_{\text{MSIFT}}(i)$ and $s^{\text{f}}_{\text{OLOF}}(i)$, $1 \le i \le N_f$ the scores of the forgery training samples of MSIFT and OLOF approach, respectively. A distance measure between the distribution of genuine and forgery scores is obtained with MSIFT approach as follows

$$\Delta_{\text{MSIFT}} = (m^{\text{g}}_{\text{MSIFT}} - m^{\text{f}}_{\text{MSIFT}})^{\text{T}} \sum (m^{\text{g}}_{\text{MSIFT}} - m^{\text{f}}_{\text{cCMSIFT}}) \tag{17}$$

where

$$m^{\text{g}}_{\text{MSIFT}} = \sum_{i=1}^{N_{\text{g}}} s^{\text{g}}_{\text{MSIFT}}/N_{\text{g}}, \qquad m^{\text{f}}_{\text{MSIFT}} = \sum_{i=1}^{N_{\text{f}}} s^{\text{f}}_{\text{MSIFT}}/N_{\text{f}}$$

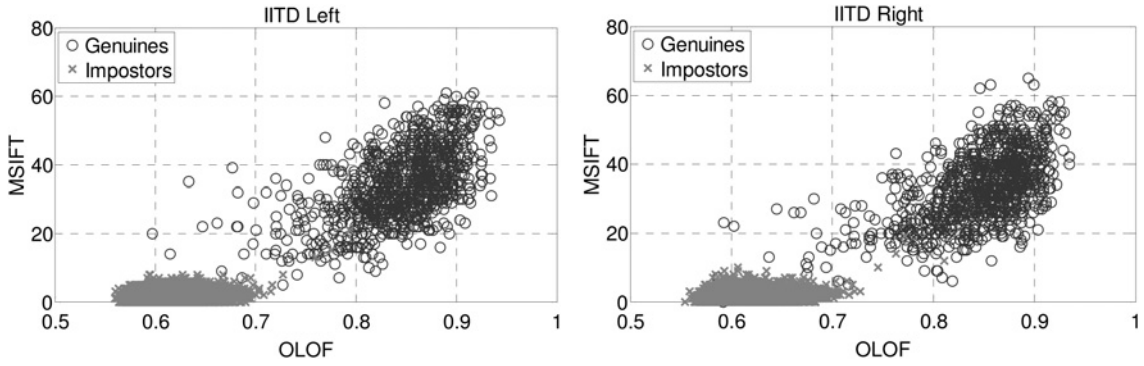

Fig. 4 *Distribution of matching scores for IITD database*

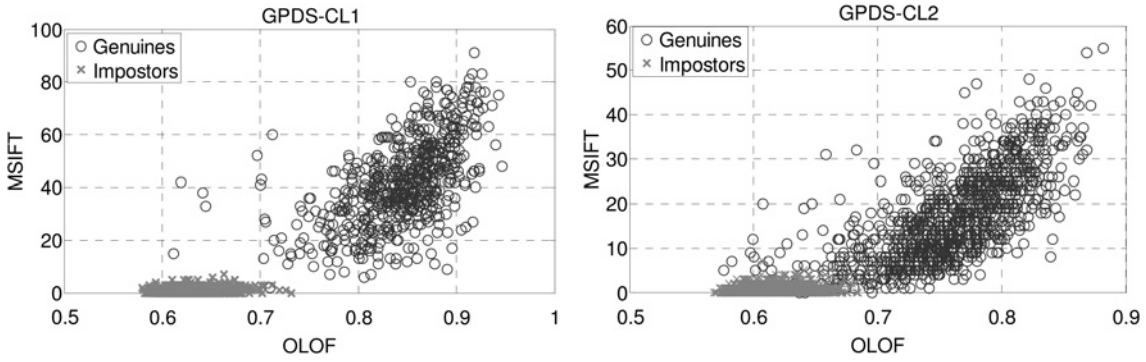

Fig. 5 *Distribution of matching scores for GPDS-CL1 database and GPDS-CL2 database*

are the means $\Sigma = (\Sigma^{g}_{MSIFT} + \Sigma^{f}_{MSIFT})/2$ with

$$\sum_{MSIFT}^{g} = \sum_{i=1}^{N_g} (s^{g}_{MSIFT}(i) - m^{g}_{MSIFT})^2/N_g \quad \text{and}$$

$$\sum_{MSIFT}^{f} = \sum_{i=1}^{N_f} (s^{f}_{MSIFT}(i) - m^{f}_{MSIFT})^2/N_f$$

the covariance matrixes. The distance between genuine and forgeries for OLOF approach Δ_{OLOF} is obtained in the same way. The weighting factor is obtained as

$$w = \Delta_{MSIFT}/(\Delta_{OLOF} + \Delta_{MSIFT}) \tag{18}$$

4 Experiments

4.1 Experimental methodology

We used the three databases as described in Table 1 to perform rigorous experiments to comparatively ascertain the performances on different scenarios. The protocols for the experiments with all the three databases are similar. The experimental results are evaluated using DET curves, equal error rates (EER), false acceptance and rejection rates (FAR and FRR, respectively). The FAR and FRR are estimated from a decision threshold estimated as a priori. A common method of estimating this decision threshold is to employ the point where the probability density function of the genuine and imposter scores intersect. Both types of scores are obtained from the training samples of all the users. In this scenario, the threshold is obtained with information of the future imposters. In real applications, the system does not have information about the imposters. Therefore we attempted to ascertain more realistic results using the decision threshold generated from using 20% of the users randomly chosen as imposter scores and the scores of the training samples of the remainder 80% of the user as genuine. Therefore the average of experimental results is estimated using the 80% of the users and by the repetition of all the experiments 10 times.

The IITD palmprint database images were acquired in single session, therefore we used all the images for the performance evaluation. We used one image for test and the rest of the five images for the training. This was repeated six times (leave one out) and the average of the experimental results is presented. Therefore the total numbers of genuine scores and imposter scores are 22 560 ($235 \times 2 \times 6 \times 0.8 \times 10$) and 5 279 040 ($235 \times 2 \times 234 \times 6 \times 0.8 \times 10$), respectively.

The GPDS-CL1 database experiments were carried out using the first five images as training set and the remaining five images as test set. Therefore the numbers of genuine scores and imposter scores are 8000 ($100 \times 10 \times 0.8 \times 10$) and 792 000 ($100 \times 99 \times 10 \times 0.8 \times 10$), respectively.

For the experiments with GPDS-CL2 database, we employed the first five images (from first session) as training samples and the rest of the images (rest of sessions) as test samples. We did not use images from different sessions for training to ascertain more realistic verification which can also account for the temporal variations introduced from time interval. Therefore the numbers of genuine scores and imposter scores are 7920 ($110 \times 9 \times 0.8 \times 10$) and 1 342 880 ($110 \times 109 \times 14 \times 0.8 \times 10$), respectively.

4.2 Comparing preprocessing techniques applied to SIFT

The use of different preprocessing techniques was evaluated in order to improve the traditional SIFT approach applied to original greyscale images. In Fig. 6 we show the different

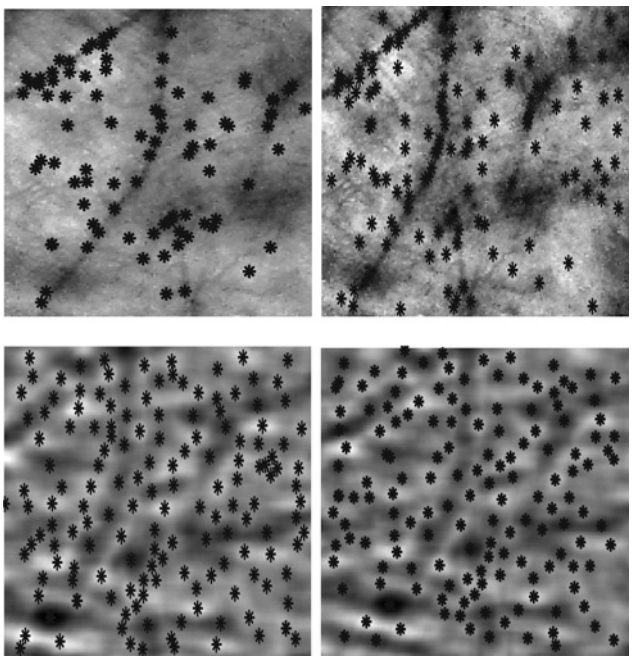

Fig. 6 *Extracted SIFT keypoints over palmprint greyscale image (upper left), palmprint image equalised by contrast limited adaptive histogram method (upper right) and palmprint preprocessed with Gaussian and Gabor filter (down left and right, respectively)*

doi: 10.1049/iet-cvi.2010.0191

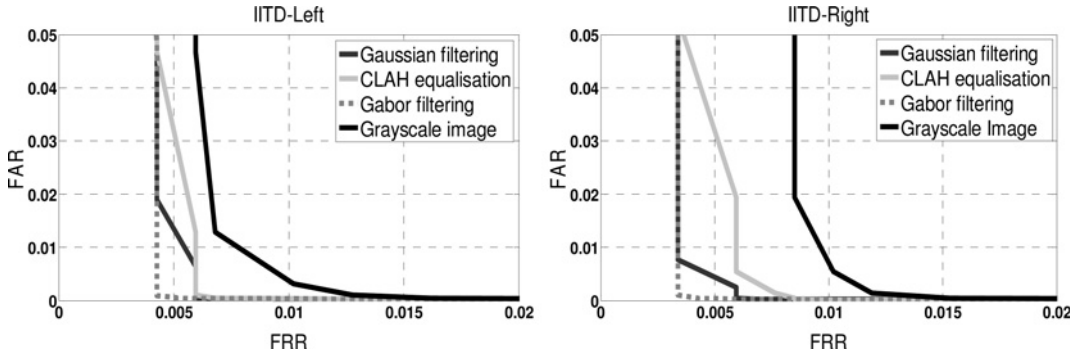

Fig. 7 *DET curves for different preprocessed techniques applied to SIFT with IITD (left) and IITD (right)*

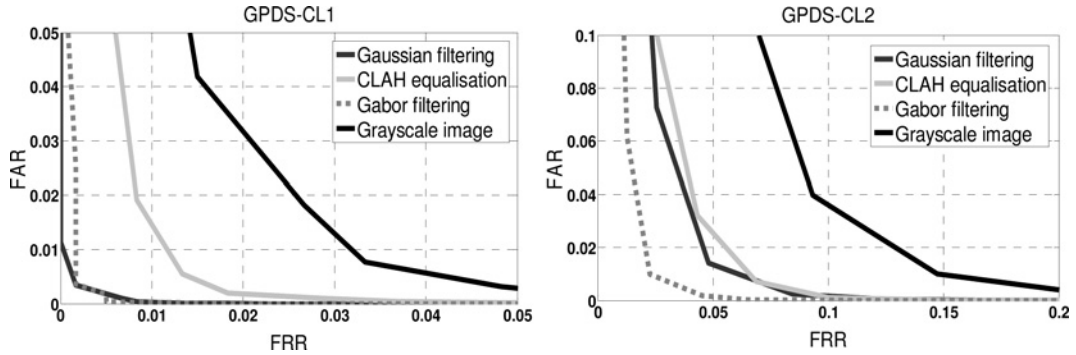

Fig. 8 *DET curves for different preprocessed techniques applied to SIFT with GPDS-CL1 (right) and GPDS-CL2 (left)*

keypoints localisation of the SIFT algorithm and the MSIFT algorithms with the three preprocessing approaches discussed in Section 3.1, that is, contrast limited adaptive histogram equalisation, Gaussian filtering and Gabor filtering.

The keypoint obtained with the SIFT algorithm on greyscale images focus the keypoints localisation on the principal lines which may not be the most distinctive information on the contactless hand images. A more uniform distribution of the keypoints over the palmprint detecting secondary lines, wrinkles and creases can significantly improve the method performance. It can be ascertained from the sample results in Fig. 6 that the usage of even Gaussian or Gabor preprocessing significantly improves the localisation of palmprint lines, wrinkles and creases.

Figs. 7 and 8 show the DET curves which compare the performance between SIFT and MSIFT based on original greyscale images and pre-processed images using, contrast limited adaptive histogram equalisation, Gaussian filtering and Gabor filtering.

All the tested pre-processing techniques outperform the results obtained with original greyscale images. Gabor outperforms Gaussian and adaptive histogram equalisation in both scenarios but this improvement is significantly better in real application scenario.

4.3 Performance comparison between OLOF and MSIFT

The experimental results are reported by using the EER, the FAR and FRR in the a priori thresholds without forger information, as shown in Tables 2–4. In Table 4 we show two different results: the results using the complete ten session images and the results using only the first session images. The results in terms of FAR and FRR obtained with a priori thresholds are not far from the EER suggesting that it is possible to estimate the thresholds without the imposter information.

Table 2 Average performance (EER) from IITD database

Matcher	EER (%)	A priori threshold	
		FAR (%)	FRR (%)
$MSIFT_R$	0.33	0.47	0.28
$MSIFT_L$	0.27	0.53	0.14
$OLOF_R$	1.31	1.51	1.12
$OLOF_L$	0.61	0.65	0.59
$Fusion_R$	0.21	0.36	0.16
$Fusion_L$	0.20	0.29	0.12

Table 3 Average performance (EER) from GPDS-CL1

Matcher	EER (%)	A priori threshold	
		FAR (%)	FRR (%)
MSIFT	0.31	0.03	0.77
OLOF	0.98	1.04	0.93
fusion	0.17	0.05	0.22

Table 4 Average performance (EER) from GPDS-CL2

Matcher	EER (%)		A priori threshold	
	1 session	10 sessions	FAR (%)	FRR (%)
MSIFT	0.43	1.39	0.61	2.31
OLOF	1.63	1.71	2.11	1.39
fusion	0.19	0.57	0.23	1.02

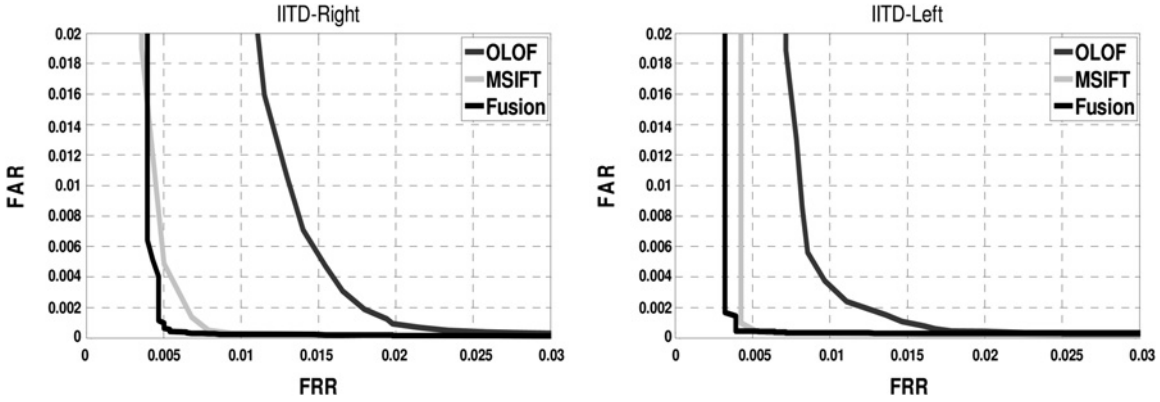

Fig. 9 *DETs curves for IITD database and OLOF, MSIFT and combination approaches*

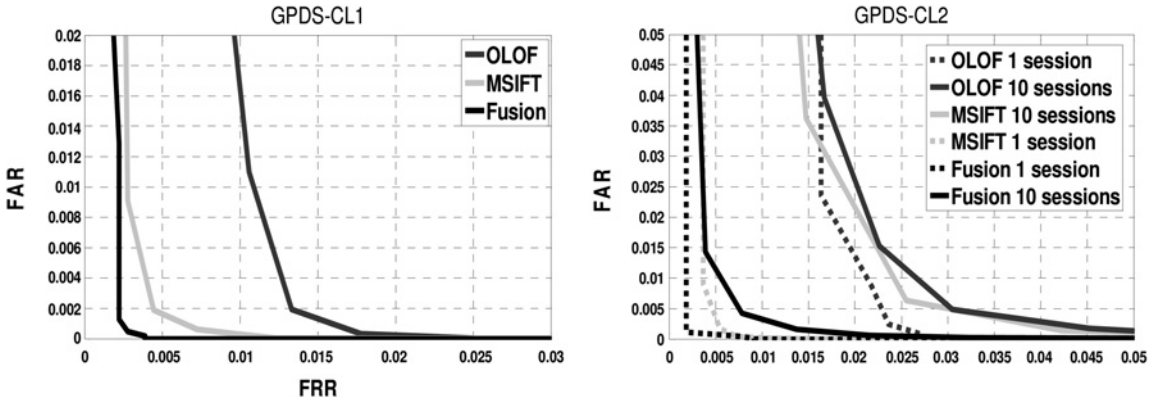

Fig. 10 *DETs curves for GPDS-CL1 database on the left and GPDS-CL2 database on the right using first session images (discontinuous line) and all session images (continuous line)*

Fig. 9 shows the DET curves from the IITD touchless palmprint database, whereas Fig. 10 illustrates the DET curves obtained from GPDS-CL1 and GPDS-CL2 databases. Concisely, The GPDS-CL2 database is composed of images from different sessions allowing a comparison between results obtained using image from one session or all sessions. Fig. 10 (left) shows the GPDS-CL1 DETs curves and Fig. 10 (right) presents two different experiments: DET curves obtained using images from the first session of GPDS-CL2 (discontinuous line) and DETs curves obtained using the complete ten session images (continuous line).

The experimental results summarised in Tables 2–4 and Figs. 9 and 10 suggest that MSIFT approach significantly outperforms OLOF approach for authentication in laboratory conditions database (IITD and GPDS-CL1) and real condition unisession and multisession database (GPDS-CL2).

The experiments done with images acquired in just one session (IITD, GPDS-CL1 an images of the first session of GPDS-CL2) produce similar results. The results obtained with the experiments done with all the images of the multisession GPDS-CL2 database show significantly differences in genuine scores distributions, see Fig. 11. In real systems with uncontrolled environments conditions the large intra-class variance produce genuine score degradation. This degradation is more obvious in MSIFT approach. Our experiments suggest that the intraclass variance (variance between images from the same user) increases significantly when the number of sessions increases, which further degrades the performance.

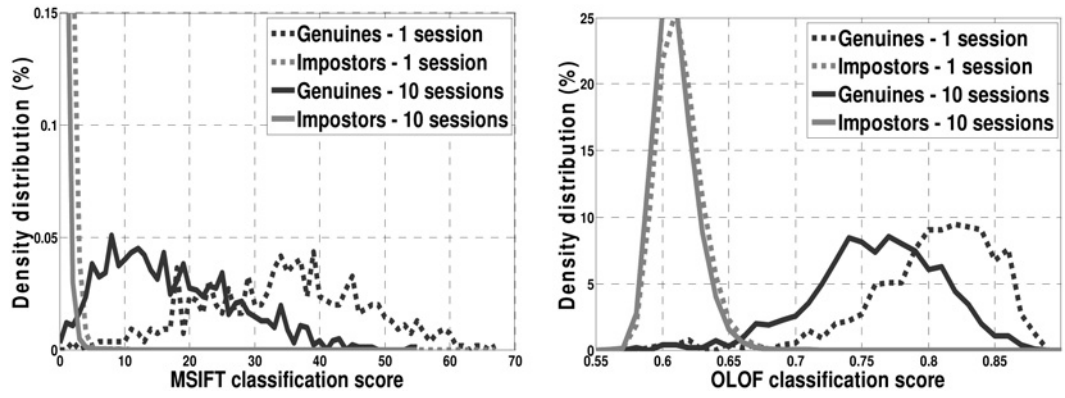

Fig. 11 *MSIFT (left) and OLOF (right) scores distribution for one session and 10 session experiments using GPDS-CL2 database*

doi: 10.1049/iet-cvi.2010.0191

On the other hand, it is important to note that the interclass variance (variance between images from different users) does not show noticeable difference when the number of sessions increases. Fig. 11 show similar impostors scores distributions for 1-session and 10-session experiments.

4.4 Robustness of MSIFT features

The better performance of MSIFT can be explained by the robustness of this feature extraction method in the presence of typically distortions associated to contactless imaging, for example, translation, rotation, scale, blurring, occlusion and projective distortions among others. In this paper we study the robustness of MSIFT and OLOF in the presence of four of the most commonly observed source of image distortions: rotation, scale, translation and occlusion.

With the above aim, after dividing the GPDS-CL1 database in training and test sets, the test set was intentionally distorted changing the scale of the images, rotate and translate them and also adding occlusion in the test set. We then comparatively evaluate the typical matching scores from such images impaired by pose changes (along with undistorted train images).

The matching scores are computed using MSIFT and OLOF approach. In the first experiment we used the test images and imparted 20% scale reduction representing inaccurate hand presentation scenario in contactless imaging. In addition, we introduced additional rotational distortion by 20° of rotation in the original image. We also simulate translation variation introducing a vertical and horizontal displacement of 20% of the images size on the original images. The occlusion is simulated by forcing to zero a region equal to the 20% of total area of the images. We repeat the experiment with all contactless palmprint images of the GPDS-CL1 database. The averaged EER obtained using MSIFT, OLOF and fusion are shown in Table 5. The first row corresponds to the EER obtained using the first four images from each user as training set and the remaining six images as test set. For the remaining rows we applied the variations to the test set. The EER obtained is a measure of the robustness of each feature approach in the presence of the most common contactless scheme variations.

The experimental results in Table 5 illustrate significant degradation in the performance of OLOF in the presence of variations resulting from rotation, translation and occlusion. With robust image segmentation methods, these distortions have a least/minor influence in traditional contact-based palmprint identification systems. In contactless schemes the presence of large pose variations increases the influence of these distortions and drastically degrades the system performance. These results attempt to ascertain why MSIFT can be more useful for the contactless palmprint images as compared to other popular palmprint approaches.

Table 5 EER robustness to contactless scenario variations

Distortion	EER	
	MSIFT, %	OLOF, %
original (no distortion)	0.31	0.98
scale (40%)	0.43	2.24
rotation (20°)	0.69	38.4
translation (20%)	0.91	26.7
occlusion (20%)	0.61	67.6

Table 6 Computational time (seconds)

Stage	Image size	MSIFT	OLOF
feature extraction	300 × 300	4.12	0.28
	150 × 150	1.81	0.07
	75 × 75	0.25	0.02
matching	–	0.007	0.25

Table 7 Related work on contactless palmprint authentication

Reference	Features	Database	Subjects	EER, %
[20]	cohort information	IITD [9]	235	1.31
[21]	palmprint directional coding	proprietary	136	1.97
[6]	2D and 3D palm features	PolyU	177	0.72
[22]	palmprint Gabor filtering	proprietary	50	8.70
[4]	multispectral palmprint OLOF	proprietary	165	0.50
this paper	MSIFT and OLOF	IITD [9]	235	0.21
		GPDS-CL1 [10]	100	0.17
		GPDS-CL2	110	0.57

4.5 Computational load

In this section we present the estimated computational time for the feature extraction and matching stages. Table 6 shows the computation time for MSIFT and OLOF feature extraction and matching on Pentium dual-core 1.66 GHz with 2 GB RAM using MATLAB 2007b. Table 6 shows the averaged run time results using the GPDS-CL1 database.

In terms of computational complexity, MSIFT approach demands more resources than OLOF approach. Although OLOF is six times faster, MSIFT approach computational time is lower than 2 s with a low performance hardware/software setting and image size of 150 × 150 pixels.

5 Conclusions

In this paper we systematically examined the contactless palmprint authentication problem and presented an analysis of resulting image variability. The MSIFT approach proposed and investigated in this paper outperforms the OLOF approach in laboratory conditions. Our experimental results on the three different contactless palmprint database suggest that the combination of MSIFT and OLOF approach offers most promising alternative for more reliable contactless palmprint authentication applications, primarily in the presence of large intraclass variations resulting from the contactless imaging in multisession and unsupervised conditions.

This paper has detailed the experiments using three different contactless palmprint databases with more than 6000 images from 680 different hands. These images were acquired in different conditions and achieve EER of 0.2% for controlled condition database (laboratory scenario) and 0.6% for uncontrolled conditions database (real application scenario). In controlled conditions with single session images, MSIFT method significantly improves the equal error rate as compared to those from OLOF method results. The reason of this improvement can be primarily attributed to the robustness of MSIFT approach against the contactless

image variations. In uncontrolled conditions with 10-session images, MSIFT and OLOF show similar performance. Working in realistic scenarios with multisession databases and uncontrolled illumination conditions is crucial to obtain realistic estimate on the results and performance. In our experiments MSIFT achieved similar performance than OLOF in real application scenario. In the presence of these large intraclass variations the combination of MSIFT and OLOF approaches offers most promising alternative.

The contactless palmprint approaches have also been studied earlier. Reference [3] presented contactless palmprint authentication but employed multispectral images and its combination to achieve performance improvement. Table 7 presents a summary of related work on contactless palmprint authentication and illustrate lack of any effort to examine the strength of MSIFT features for contactless imaging. This paper has presented such experiments with promising results. Our further research efforts are focused to exploit the colour information, which can also be simultaneously extracted during contactless palmprint imaging, and develop discriminant models to effectively assist in more reliable contactless palmprint identification. Another research direction is to explore the fusion with other uncorrelated biometrics as contactless finger geometry features which can also be simultaneously acquired from the contactless hand images.

6 Acknowledgments

This work has been funded by Spanish government MCINN TEC2009-14123-C04 research project.

7 References

1 Jain, A.K., Ross, A., Pankanti, S.: 'A prototype hand geometry-based verification system'. Proc. 2nd Int. Conf. on Audio- and Video-Based Biometric Person Authentication, March 1999, pp. 166–171
2 Amayeh, G., Bebis, G., Erol, A., Nicolescu, M.: 'Hand-based verification and identification using palm-finger segmentation and fusion', *Comput. Vis. Image Understand.*, 2009, **113**, pp. 477–501
3 Kanhangad, V., Kumar, A., Zhang, D.: 'A unified framework for contactless hand verification', *IEEE Trans. Inf. Foren. Secur.*, 2011, **6**, (3), Part 2, pp. 1014–1027
4 Hao, Y., Sun, Z., Tan, T., Ren, C.: 'Multi-spectral palm image fusion for accurate contact-free palmprint recognition'. Proc. IEEE Int. Conf. on Image Processing, ICIP 2008, 2008, pp. 281–284
5 Morales, A., Ferrer, M.A., Alonso, J.B., Travieso, C.M.: 'Comparing infrared and visible illumination for contactless hand based biometric scheme'. Proc. 42nd Annual IEEE Int. Carnahan Conf. on Security Technology, ICCST 2008, 2008, pp. 191–197
6 Kanhangad, V., Kumar, A., Zhang, D.: 'Contactless and pose invariant biometric identification using hand surface', *IEEE Trans. Image Process.*, 2011, **20**, (5), pp. 1415–1424
7 Morales, A., Ferrer, M.A., Kumar, A.: 'Improved palmprint authentication using contactless imaging'. Proc. Fourth IEEE Int. Conf. on Biometrics Theory, Applications and Systems, BTAS 2010, Washington, September 2010
8 Sun, Z., Tan, T., Wang, Y., Li, S.Z.: 'Ordinal palmprint representation for personal identification'. Proc. IEEE Computer Society Conf. on Computer Vision and Pattern Recognition, 2005, vol. 1, pp. 279–284
9 IITD Touchless Palmprint Database, version 1.0, http://web.iitd.ac.in/~ajaykr/Database_Palm.htm
10 GPDS-CL1 Database, http://www.gpds.ulpgc.es
11 Ferrer, M.A., Morales, A., Travieso, C.M., Alonso, J.B.: 'Low cost multimodal biometric identification system based on hand geometry, palm and finger print texture'. Proc. 41st Annual IEEE Int. Carnahan Conf. on Security Technology, 2007, pp. 52–58
12 Lowe, D.G.: 'Distinctive image features from scale-invariant keypoints', *Int. J. Comput. Vis.*, 2004, **2**, (60), pp. 91–110
13 Badrinath, G.S., Gupta, P.: 'Palmprint verification using sift features'. Proc. First Workshops on Image Processing Theory, Tools and Application, IPTA 2008, 2008, pp. 1–8
14 Zuiderveld, K.: 'Contrast limited adaptive histogram equalization', Graphic Gems IV (Academic Press Professional, San Diego, 1994), pp. 474–485
15 Zhang, D., Kong, W., You, J., Wong, M.: 'Online palmprint identification', *IEEE Trans. Patt. Anal. Mach. Intell.*, 2003, **25**, (9), pp. 1041–1050
16 Hennings, P., Kumar, V.: 'Palmprint classification using multiple advanced correlation filters and palm-specific segmentation', *IEEE Trans. Inf. Foren. Secur.*, 2007, **2**, (3), pp. 613–622
17 Kong, W.K., Zhang, D.: 'Competitive coding scheme for palmprint verification'. Proc. 17th Int. Conf. on Pattern Recognition, 2004, vol. 1, pp. 520–523
18 Nandakumar, K., Chen, Y., Dass, S.C., Jain, A.K.: 'Likelihood ratio based biometric score fusion', *IEEE Trans. Patt. Anal. Mach. Intell.*, 2008, **30**, pp. 342–347
19 Jain, A.K., Nandakumar, K., Ross, A.: 'Score normalization in multimodal biometric systems', *Patt. Recogn.*, 2005, **38**, pp. 2270–2285
20 Kumar, A.: 'Incorporating cohort information for reliable palmprint authentication'. Proc. Sixth Indian Conf. on Computer Vision, Graphics & Image Processing, Bhubaneswar (India), December 2008, pp. 112–119
21 Michael, G.K.O., Connie, T., Jin, A.T.B.: 'An innovative contactless palmprint and knuckle print recognition system', *Patt. Recogn. Lett.*, 2010, **31**, (12), pp. 1708–1719
22 Methani, C., Namboodiri, A.M.: 'Pose invariant palmprint recognition'. Proc. Third Int. Conf. on Biometrics, ICB 2009, June 2009, pp. 577–586

doi: 10.1049/iet-cvi.2010.0191